Available online at www.sciencedirect.com

ScienceDirect

materialstoday: PROCEEDINGS

Materials Today: Proceedings 3 (2016) 889 – 897

12th International Conference on Nanosciences & Nanotechnologies & 8th International Symposium on Flexible Organic Electronics

Biomedical Co-Cr-Mo components produced by Direct Metal Laser Sintering ★

E.Girardin[1]*, G. Barucca[2], P.Mengucci[2], F.Fiori[1], E.Bassoli[3], A.Gatto[3], L. Iuliano[4], B. Rutkowski[5]

[1]*DISCO, Università Politecnica delle Marche, Via Brecce Bianche, 60131 Ancona, Italy*
+39 0712204603, e.girardin@univpm.it
[2]*SIMAU, Università Politecnica delle Marche, via Brecce Bianche, 60131 Ancona, Italy*
[3]*DIMeC, University of Modena and Reggio Emilia, via Vignolese 905/B, Modena 41125, Italy*
[4]*DISPEA, Politecnico di Torino, C.so Duca degli Abruzzi 24, 10129 Torino, Italy*
[5] International Centre of Electron Microscopy for Materials Science, AGH University of Science and Technology, al. A. Mickiewicza 30, 30-059 Krakow, Poland

Abstract

Direct Metal Laser Sintering (DMLS) is an additive manufacturing technique based on a laser power source that sinters powdered materials using a 3D CAD model. The mechanical components produced by this procedure typically show higher residual porosity and poorer mechanical properties than those obtained by traditional manufacturing techniques. In this study, samples were produced by DMLS starting from a Co-Cr-Mo powder (in the γ phase) with a composition suitable for biomedical applications. Samples were submitted to hardness measurements and structural characterization. The samples showed a hardness value remarkably higher that those commonly obtained for the same cast or wrought alloys. In fact, the HRC value measured for the samples is 47 HRC, while the usual range for CAST Co-Cr-Mo is from 25 to 35 HRC. The samples microstructure was investigated by X-ray diffraction (XRD), electron microscopy (SEM and TEM) and energy dispersive microanalysis (EDX) in order to clarify the origin of this unexpected result. The laser treatment induced a melting of the metallic Co-Cr-Mo powder, generating a phase transformation from the γ (fcc) to the ε (hcp) phase. The rapid cooling of the melted powder produced the formation of ε (hcp) nano-lamellae inside the γ (fcc) phase. The nano-lamellae formed

* Corresponding author. Tel.: +39 071 2204603; fax: +39 071 2204605.
E-mail address: e.girardin@univpm.it

Selection and peer-review under responsibility of the Conference Committee Members of NANOTEXNOLOGY2015 (12th International Conference on Nanosciences & Nanotechnologies & 8th International Symposium on Flexible Organic Electronics)
doi:10.1016/j.matpr.2016.02.022

an intricate network responsible for the measured hardness increase. The results suggest possible innovative applications of the DMLS technique to the production of mechanical parts in the medical and dental fields, where a high degree of personalization is required.

Selection and peer-review under responsibility of the Conference Committee Members of NANOTEXNOLOGY2015
(12th International Conference on Nanosciences & Nanotechnologies & 8th International Symposium on Flexible Organic Electronics)

Keywords: biomedical alloy; laser sintering; mechanical properties; Transmission electron microscopy; Scanning electron microscopy; X-ray diffraction

1. Introduction

The need to create superior products that demonstrate great mechanical integrity is a timeless challenge. In today's world, there is a growing need to produce devices, parts, and systems for a variety of industries within a short period and a limited budget. The devices used in the medical and dental industries are often geometrically complex and require faithful adherence to design specifications. Fortunately, with innovative new technologies like direct metal laser sintering (DMLS), complex parts can be fabricated quickly and accurately.

Direct metal laser sintering (DMLS) is an additive manufacturing (AM) technique that uses a laser as the power source to sinter powdered material, aiming the laser automatically at points in space defined by a 3D model, binding the material together to create a solid structure. Inside the build chamber area, there is a material dispensing platform and a build platform along with a recoater blade used to move new powder over the build platform. The technology fuses metal powder into a solid part by melting it locally using the focused laser beam. Parts are built up additively layer by layer, typically using layers 20 micrometres thick. This process allows for highly complex geometries to be created directly from the 3D CAD data, fully automatically, in hours and without any tooling. This technology is used to manufacture direct parts for a variety of industries including aerospace, dental, medical and other industries that have small to medium size, highly complex parts and the tooling industry to make direct tooling inserts. DMLS is a very cost and time effective technology. The technology is used both for rapid prototyping, as it decreases development time for new products, and production manufacturing as a cost saving method to simplify assemblies and complex geometries.

In the recent past years, AM techniques were used to produce biomedical parts, in particular to produce biocompatible Co-based alloys. Cast cobalt-base alloys were originally proposed for surgical implants over 60 years ago. Cast Co-26Cr-6Mo medical implants such as hips, knees and bone plates were typically used. The combination of high strength and toughness makes metals the first choice for loading–bearing applications [1, 2]. Among various metallic biomaterials, Co-Cr-Mo alloy is one of the most attractive solutions [3-5]. This alloy can be ALMed through Direct Metal Laser Sintering (DMLS), which exhibits a high potential in the field of rapid manufacturing (RM) [6, 7]. In the field of dental restorations, metal-ceramic fixed partial dentures (FPDs) can be produced by DMLS with a strong reduction of manual operation and accordingly higher repeatability and good savings in money and delivery times [7]

DMLS has the potentiality to substitute traditional techniques for the production of prostheses, but the full benefits of ALM in prosthetics require specific design, implementation and evaluation, to address the requirements of the field [8]. DMLS is a complex process where a large number of factors are involved and a strong theoretical basis is still lacking [9, 6]. Many experimental characterizations are available [10–12] and some authors studied the physics of heat supply and transfer during consolidation [13-15], but a comprehensive model accounting for parts' performances and microstructure is not available yet. The mechanical properties of the sintered components are strictly linked to the samples microstructure and are one of the major aspects connected to the practical applications of the AM procedures. Usually, objects produced by metal powder sintering show poorer mechanical properties than those produced by conventional procedures. This behaviour is mainly due to the fact that DMLS, depending on the laser energy density employed, involves a partial or total melting of the powder. Therefore, the products made by DMLS could show high surface roughness, porosity (in certain cases even lack of densification), heterogeneous

microstructure and thermal residual stresses, that may give rise to poor mechanical properties [16].

In this paper, metallic samples of a biocompatible Co-Cr-Mo alloy produced by the DMLS technique were deeply investigated in order to correlate their mechanical properties to the corresponding microstructure. To this aim, the mechanical performances, X ray diffraction (XRD) analysis, electron microscopy (SEM, TEM) observations and energy dispersive microanalysis (EDX) were performed on the samples.

2. Materials and methods

2.1. Material composition and sintering parameters

Tensile samples were produced by DMLS following ASTM E8M specifications for flat unmachined specimens from powder metallurgy (Fig. 1) using a a Yb-fibre laser system on EOSINT-M270 with the standard parameters reported in Table 1.

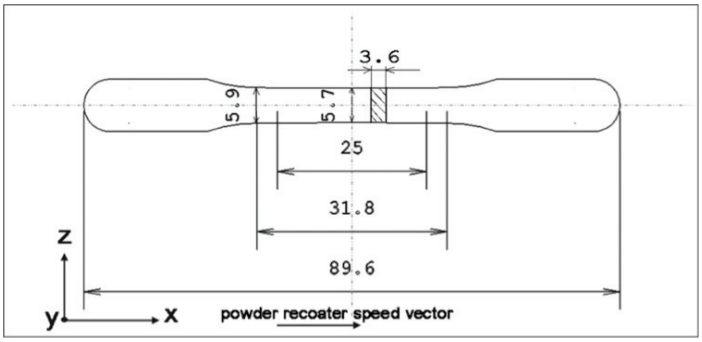

Fig. 1. Geometry of the tensile specimens

Table 1. DMLS sintering parameters

Laser power	200 W
Laser spot diameter	0.200 mm
Scan speed	Up to 7.0 m/s
Building speed	2-20 mm^3/s
Layer thickness	0.050 mm
Protective atmosphere	Max 1.5% oxygen

Every layer is built with a specific strategy to minimize secondary anisotropy. The slice area is divided into squares of 4 mm side, built one next to the other. After every square's building the laser spot is realigned. On each layer the laser acts with parallel wipes directed according to a definite scan vector. For the next layer the scan vector is rotated by 25° with respect to the previous one. Within the plane of powder deposition, the described laser path should ensure isotropic consolidation phenomena and the only distinction between the two main axes is related to powder laying, since the recoater moves along the X direction. To verify the above assumptions specimens in both alloys are produced (4 for each group) in three orientations with respect to the machine distinctive directions.

- "0" group: specimens' axis parallel to the X direction in the machine building volume, i.e. to the powder re-coater speed vector (Fig. 1);
- "90" group: specimens' axis parallel to the Y direction, i.e. perpendicular to X;
- "45" group: specimens' axis parallel to the bisector of the X-Y quadrant.

The powder used as raw material is the EOS Cobalt/Chrome SP2 cobalt based metal ceramic alloy designed for production of Porcelain-Fused to Metal (PFM) dental prosthesis (crowns, bridges, etc.) in EOSINT M 270 Standard installation mode. The powder is class IIa medical device in accordance with annex IX rule 8 of the MDD 93/42/EEC. Composition corresponds to "type 4" CoCr dental material according to EN ISO 22674.
The nominal composition, provided by the manufacturer (EOS GmbH Electro Optical Systems), is given in Table 2.

Table 2. Nominal composition of the Co-Cr-Mo alloy

wt.%				
Co	Cr	Mo	Si	W
63.8	24.7	5.1	1.0	5.4

2.2. Mechanical testing

The specifications of ISO 4498 (Sintered metal materials, excluding hardmetals - Determination of apparent hardness and microhardness) were applied to perform Rockwell C measurements, which are performed following ISO 6508 (Rockwell hardness test), five tests on each sample.

Ultimate Tensile Strength (UTS) tests were performed using an elongation speed of 5mm/min, on SCHENK (HYDROPULS PSB) testing machine, with a load cell acting up to 250 kN. Results were elaborated through statistical tools and the presence of significant differences between the groups was assessed by the t-test with a level of significance of 0.05.
Metallographic etching has been carried out using Dix-Keller's reagent (HF 2% vol, HCl 1,5 % vol, HNO_3 2,5 % vol; water bal.) for Ti6Al4V and electrochemical etching (HCl 0,1 M, 2V, 2 min.) for the Co-Cr-Mo alloy. Etched surfaces were then observed with SEM to investigate microstructures.

The analysis was extended at the nano-scale by using X-ray diffraction and TEM observation.

3. Results

3.1. Mechanical tests

3.1.1 Hardness

The average Rockwell C Hardness (HRC) value measured for the laser sintered sample is 47 (Table 3). This result is surprisingly high with respect to the value reported in literature.

Table 3. Rockwell C Hardness (HRC)

	HRC
CoCrMo 0	46.9
CoCrM0 45	46.9
CoCr Mo 90	47.0
Literature	25-35

3.1.2 Ultimate Tensile Strength

As to Co-Cr-Mo parts, mean UTS was about 1280-1300 MPa, with elongations in the range 12.8 to 14%. All groups proved to have good test repeatability with a very low standard deviation (Table 4). Regarding tensile

strength, there are not significant differences between the groups if a significance of 95% is assumed, but a light increase can be noticed from “0” to “45” and “90” groups. The t-test on UTS between “0” and “90” groups provides a p-value of 0.06, only slightly above the adopted confidence level. Considering elongation instead, there are significant differences between “45” group and the other two directions.

Table 4. Ultimate Tensile Strength and Elongation at break

	UTS (MPa)		**ε_b (%)**	
	Mean	**SD**	**Mean**	**SD**
CoCrMo 0	1281	12.80	12.81	0.45
CoCrMo 45	1290	12.81	14.09	0.22
CoCrMo 90	1301	14.09	13.00	0.72
Literature	700-800		8-11	

3.2. X-ray diffraction

X-ray diffraction measurements were performed on both the Co-Cr-Mo powder used for the sintering process, and on the sintered sample (Fig. 2).

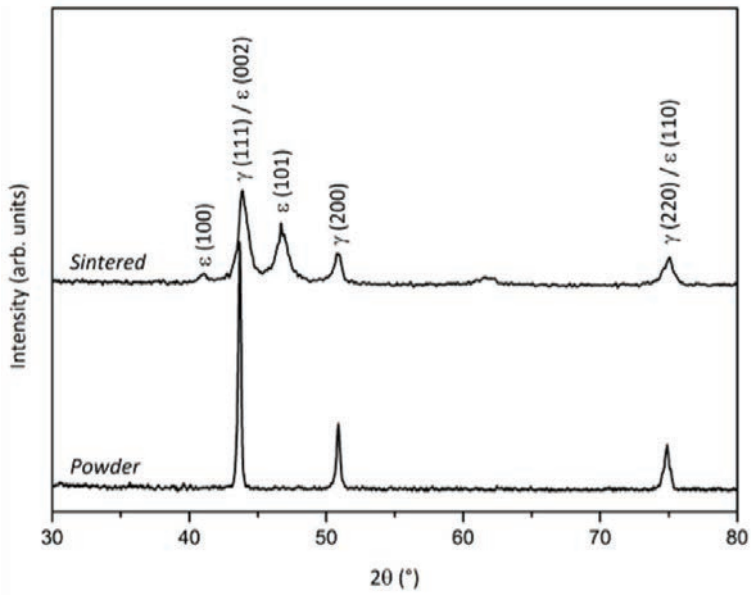

Fig. 2. X-ray diffraction patterns of the Co-Cr-Mo powder and the sintered sample

The diffraction pattern of the as-received powder is reported in Fig. 2. The visible diffraction peaks identify the cubic cobalt phase, also referred as γ phase (fcc). Each diffraction peak is indexed with the corresponding family of lattice planes. The fcc γ phase has a nominal lattice parameter a=0.35447 nm (ICDD card n.15-806). After fitting the diffraction peaks of Fig. 2, the lattice parameter of the powder is found to be a=0.3586 nm, in good agreement with the values reported in literature for alloys of similar composition [17].

The diffraction pattern of the sintered sample is also shown in Fig. 2. The most intense and sharp diffraction peaks are a result of the presence of both γ and ε cobalt phases. The ε phase has a hexagonal closed packed (hcp)

lattice with nominal parameters a=0.25031 nm and c=0.40605 nm (ICDD card n. 5-727). Determining the lattice parameters of our alloy from the ε (100) and (101) peaks, we obtained in the hexagonal ε phase a=0.2539 nm and c=0.4122 nm with a c/a ratio of 1.623. The lattice parameters of the cubic γ phase in the sintered sample, obtained from the γ (200) peak, resulted in a=0.3589 nm. Experimental results are in good agreement with the values reported in literature [17].

The volume fraction of the hexagonal ε phase was determined using the Sage and Gillaud's method [18], by estimating the integrated intensities of the γ (200) and ε (101) peaks. It was found an ε phase volume fraction $f_{hcp}=0.49 \pm 0.03$.

3.3. Scanning electron microscopy (SEM)

Scanning electron microscopy observations were performed on both the as-received powder and the sintered specimens (Fig. 3). From the SEM images the average size of the particles was evaluated between 4 to 50 μm.

The etched sections in Fig. 3(a) show a peculiar macro-structure, similar to "fish scales", relative to the weld pools of each laser pass and to layer stack. AM growth direction can be identified, vertical in the images. Higher magnifications show that inside the described domains an extremely fine microstructure is present. Columnar grains with diameters in the range 300-400 nm and heights more than ten times higher (4-8 μm) can be observed, growing perpendicular to the melt pool boundary, because of heat transfer. An ultra-fine-grained material is obtained by AM, which accounts for the very high strength of these specimens (Fig. 3(b)).

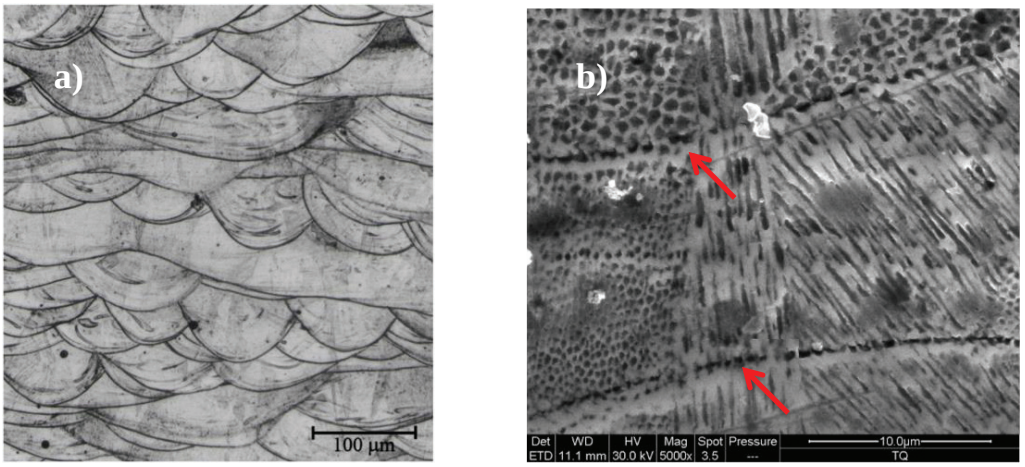

Fig. 3. SEM image of the sintered sample (a) "fish scales" structure (b) weld pools (red arrows) and columnar structure

3.4. Transmission electron microscopy (TEM)

TEM observation of the sintered samples confirms the co-presence of the ε (hcp) and γ (fcc) phases. The ε phase forms as small lamellae inside the γ phase (Fig. 4).

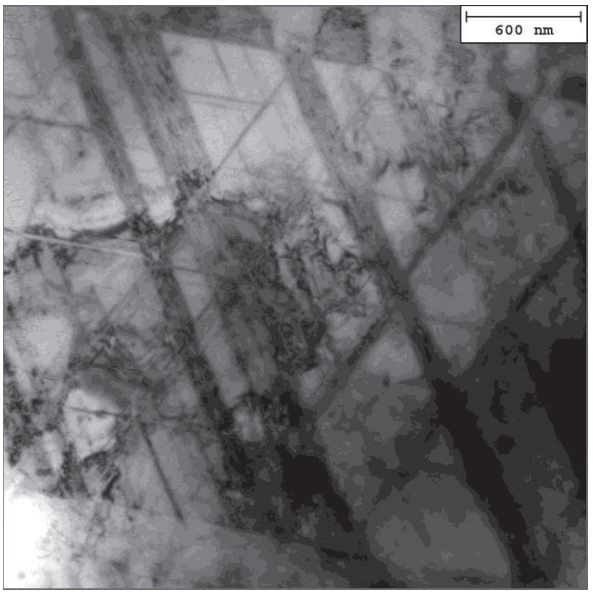

Fig. 4. TEM bright field image of the ε lamellae inside the γ phase taken in the <111> γ zone axis orientation

Figure 5 identifies clearly the two cobalt phases and the lamellar structure. Performing the Fourier transform (FFT) of the selected areas, two diffraction patterns are obtained and reported in the inserts. The thickness of the lamellae is about few nanometers. The ε lamellae tend to aggregate and form the columnar structure observed in the SEM images.

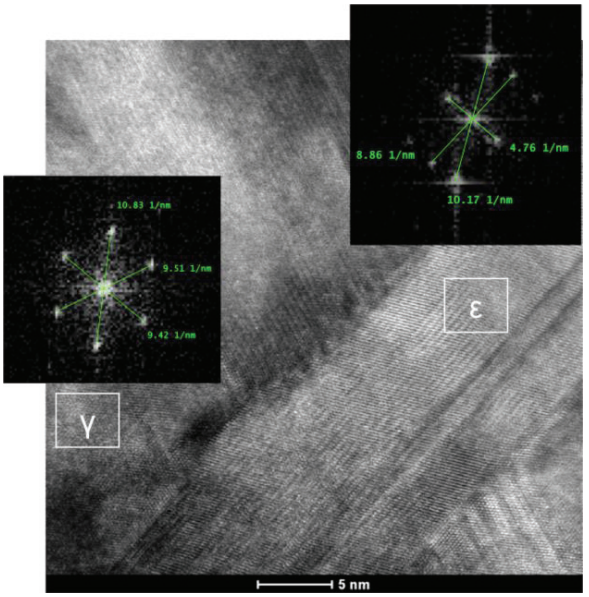

Fig. 5. High resolution image of the sample

From the selected area diffraction (SAED) patterns (not shown here) taken in different zone axis orientation and the high-resolution images, it is possible to deduce the following orientation relationships:

$$\{001\}_\varepsilon \,//\, \{111\}_\gamma$$
$$<100>_\varepsilon \,//\, <1\text{-}10>_\gamma$$

It is observed that the ε lamellae grow on the $\{111\}_\gamma$ lattice planes [19].

4. Discussion

The hardness value obtained from the sintered samples is surprisingly high with respect to the value reported in literature. In general, components produced by Additive Manufacturing present high porosity and, as consequence, poor mechanical properties. Typically, components produced with traditional manufacturing methods exhibit better mechanical properties. On the contrary, the Ultimate Tensile Strength and the Elongation at break values obtained from the sintered samples are higher than the ones reported in literature [20] and confirm a mechanical anisotropy. These results can be explained by the observed microstructure of the specimens and will be discussed in more details below.

X-ray diffraction shows that the powder consists only of the γ (fcc) cobalt phase and confirms in the sintered samples the typical structure of such Co based alloys with the presence of both γ (fcc) and ε (hcp) phases. The two phases are known to be stable above 970°C and at room temperature, respectively [21]. The phase transformation from fcc to hcp can occur athermally by rapid cooling [18]. In such a production technique, the laser operates locally and on a small area; it melts the metal that solidify quickly. The laser treatment induces this athermal phase transformation from γ (fcc) to ε (hcp).

SEM observations highlight the peculiar structure of the DMLS samples. The structure described in SEM images can be identified as ε (hcp) lamellae of 1-2 nm dispersed in the γ (fcc) phase which aggregate, forming the columnar structures inside a same weld pool. Relative orientation between the two phases is constant in the sample.
TEM observations confirms the compresence of both ε (hcp) and γ (fcc) cobalt phases, with ε lamellae inside the γ matrix. The hexagonal lamellae grow on the slip planes {111} of the cubic phase. X-ray diffraction allowed to calculate the ε phase volume fraction in the sample, which resulted to be 49%, and is in agreement with the SEM and TEM observations.

The high mechanical properties observed for the sintered alloy are due to the presence of ε-lamellae growing on the $\{111\}_\gamma$ planes that limits the dislocations slip in the γ (fcc) phase.

5. Conclusion

Direct Metal Laser Sintering has been used to produce Co-Cr-Mo components for dental application. The sintered samples present a composition and microstructure suitable for biomedical application.
The processing parameters used in the DMLS process resulted in samples with a peculiar intricate network of ε lamellae inside the γ phase. The ultimate tensile strength, the elongation at break and the hardness values are superior to the ones obtained for the components produced with traditional techniques. These excellent mechanical properties are due to the particular microstructure of the samples. DMLS technique proves to be adapted for the production of biomedical implants, as it allows to produce implants especially designed for a particular patient, with sizes, shapes, and mechanical properties optimized, for different areas of medicine.

Acknowledgements

The authors wish to acknowledge the support of the COST Action MP1005. The research leading to these results has received funding from the European Union Seventh Framework Programme under grant agreement 312483 - Esteem2 (integrated infrastructure initiative–I3).

References

[1] A. Eliasson, CF. Arnelund, A. Johansson, J. Prosthet Dent. Jul.98 (1) (2007) 6-16
[2] Howards W. Roberts, David W. Berzins, B. Keith Moore, David G. Charlton, Journal of Prosthodontics 18(2) (11/2008)188- 94.
[3] B. Vandenbroucke, J.-P. Kruth, Rapid Prototyping Journal, 13(4) (2007) 196-203
[4] M. Gradzka-Dahlke, J.R. Dabrowski, B. Dabrowski, Journal of Materials Processing Technology, 2204(1-3) (2008)199-205
[5] Xiang Li, Chengtao Wang, Wenguang Zhang, Yuanchao Li, Materials Letters, 63(3-4) (2009) 403-405
[6] P. Fischer, V. Romano, H.P. Weber, N.P. Karapatis, E. Boillat R. Glardon, Acta Materialia, 51 (2003) 1651–1662.
[7] J.R. Strub, E.D. Rekow, S. Witkowski, J. Am. Dent. Assoc., 137 (2006) 1289-1296
[8] R. Bibb, D. Eggbeer, P. Evans, Rapid Prototyping Journal, 16(2) (2010) 130-137
[9] M. van Elsen, F. Al-Bender, J.-P. Kruth, Rapid Prototyping Journal, 14(1) (2008) 15-22
[10] A. Simchi, Materials Science and Engineering A, 428 (1-2) (2006) 148-158
[11],J.-P. Kruth, P. Mercelis, J. Van Vaerenbergh, L. Froyen, M. Rombouts, Rapid prototyping journal, 11 (2005) 26-36
[12] N. Tolochko et al., Rapid Prototyping J. 9(2) (20013) 68-78
[13] P. Fischer, M. Locher, V. Romano, H. P. Weber, S. Kolossov, R. Glardon, International Journal of Machine Tools and Manufacture, 44(12-13) (2004) 1293-1296
[14] P. Fischer, N. Karapatis, Appl. Phys., A74 (2002) 467–474
[15] A.V. Gusarov, T. Laoui, L. Froyen , V.I. Titov,, Journal of Heat and Mass Transfer, 46 (2003) 1103–1109
[16] C. Sanz, V.G. Navas, J. Mater. Process. Technol., 213 (2013) 2126-2136
[17] A.J. Saldivar-Garcia, H.F. Lopez, Scripta Mater. 45 (2001) 427-433
[18] J.S. Garcia, M.A. Medrano, A.S. Rodriguez, Metall. Mater. Trans. A 30 (1999) 1177-1184
[19] G. Barucca et al., Materials Science and Engineering C 48 (2015) 263-269
[20] M. Semlitsch, Eng. Med. 9 (1980) 201-207
[21] A.J. Saldivar-Garcia, M.A. Mani, R.A. Salinas, Scr. Mater. 40 (1999) 717-722